Quenching studies of pyrenoyl glutamic acid derivatives

Sanjukta Aich and Heinz-Bernhard Kraatz*

Department of Chemistry, University of Saskatchewan, 110 Science Place, Saskatoon, SK, Canada, S7N 5C9. E-mail: kraatz@skyway.usask.ca; Phone: (306) 966-4660; Fax: (306) 966-4730

Received (in Gainesville) 27th July 1998, Accepted 9th November 1998

The preparation and full characterization of fluorescent labeled *N*-pyrenoyl–L-glutamic acid diethyl ester (**2**) and 4-(*N*-Boc–L-glutamide(*O*-benzyl ester))–*N*,*N*-dimethylaniline (**3**) by the DCC–HOBT protocol is described. The benzyl group in **3** was removed by hydrogenation giving the free acid 4-(*N*-Boc–L-glutamide(OH))–*N*,*N*-dimethylaniline (**4**). The steady-state and time-resolved fluorescence quenching studies were performed in order to distinguish ground state quenching taking place in a hydrogen-bonded complex and dynamic quenching. Weak molecular interactions between the fluorophore **2** and the quencher **4** leading to a 1 : 1 complex were detected by ^{1}H-NMR titration experiments. The association constants were determined by fluorescence methods to be in the order of 3.8–4.0 × 10^3 M^{-1} for all systems investigated. The bimolecular quenching constants k_q are in the order of 1.0–1.28 × 10^{10} M^{-1} s^{-1}, indicating a diffusion controlled electron transfer process.

Introduction

Electron transfer (ET) is key to many biological processes, ranging from the utilization of light in green plants to the reduction or oxidation of bound substrates in enzymatic systems.[1] ET often proceeds through a complex system containing various structural elements, such as β-sheets and α-helices and other bonding and non-bonding contacts. According to theoretical studies by Beratan and co-workers,[2a,b] peptides having a β-sheet structure are more effective in mediating ET than α-helices. If however hydrogen bonding is present the ET rates of α-helices will be greatly enhanced, indicating the crucial role the H-bonding plays in facilitating through-protein electronic coupling.[2]

Recently, studies by Therien,[3] Nocera[4] and Hamilton[5] on well-defined donor–acceptor systems, possessing a hydrogen bonded linkage between the donor and the acceptor, have clearly demonstrated the importance of the H-bonded interface in influencing electron transfer (ET) processes. Although there are experimental studies of ET processes in well-defined peptidic systems,[6] studies of peptides where the ET proceeds through the H-bonded interface are currently not available.

In H-bonded peptidic systems, we have to consider at least four possible H-bonded interfaces. The carboxylic acid bridge (**A**), the guanidinium–carboxylate salt bridge (**B**), such as the Glu–Arg or Asp–Arg salt bridges, and the interaction of an acid sidechain with the peptide backbone (**C**) are mainly responsible for intramolecular and intermolecular binding, whereas the backbone interaction **D** is the structural motif of β-sheets.[7]

We decided to make use of the ability of carboxylic acids to form hydrogen bonded dimers in non-hydrogen bonding high polarity solvents, such as acetonitrile, in order to evaluate the ET properties of labeled amino acids capable of H-bonding. Our goal in this study was to provide evidence for efficient ET from a donor to an acceptor moiety through the H bonded interface in a peptidic model system, addressing interactions of types **C** and **D** involving the peptidic backbone. In this study, we decided to link photoactive donors and acceptors to simple amino acid subunits. We chose the well-studied 4-amino-*N*,*N*-dimethylaniline–pyrene (adma–pyr) donor–acceptor couple[8] for our studies and chose to link these to glutamic acid and study their fluorescence quenching behaviour. The pyr and adma moieties can be conveniently attached to protected glutamic acid derivatives using the DCC–HOBT protocol.[9] After deprotection of the Glu sidechain, the systems can be evaluated for their H-bonding behavior in solution. In our studies, it is necessary to evaluate the static and dynamic quenching behavior of all systems, since we will have to distinguish ground-state quenching, taking place in an H-bonded complex, from collisional dynamic quenching.

In this study we wish to report synthetic procedures for the modifications of the pyrene fluorophore and the adma quencher with glutamic acid derivatives. Furthermore, we will detail our results on the steady-state and time-resolved fluorescence studies of several pyrenoyl–glutamic acid derivatives in the absence and presence of modified adma quenchers. Experimental results will be compared with theoretical calculations based on Marcus theory.[10]

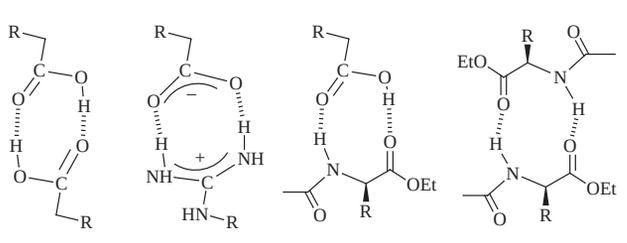

A **B** **C** **D**

Chart 1

Experimental

For synthetic purposes all solvents (BDH) were used without further purification. For spectroscopic studies, acetonitrile was dried over CaH_2 and freshly distilled under nitrogen prior to use. DCC, HOBT, pyrene-1-carboxylic acid (Aldrich) and 4-amino-*N*,*N*-dimethylaniline (adma) dihydrochloride (Fluka) were used as received. The protected amino acids Boc–Glu(OBzl)–OH (Calbiochem, Advanced ChemTech) and H–Glu(OEt)–OEt (Aldrich) were used as received.

^{1}H and ^{13}C NMR were recorded on a Bruker AMX-300 instrument at 300.135 and 75.478 MHz respectively. All chemical shifts (δ) are reported in ppm and coupling constants

(J) in Hz, relative to tetramethylsilane and are referenced to the residual signal of $CHCl_3$ (δ 7.27). Spectral assignments were made using 135-DEPT (distortionless enhancement by polarization transfer), by 2D-COSY and HMQC. Absorption spectra were recorded using a Hewlett Packard (845OA) spectrophotometer.

Fluorescence studies

Fluorescence studies were carried out in a SPEX FLUOROLOG (Model 1680) fluorescence spectrometer at the corresponding absorption maxima of the fluorophores (see Table 1). Similar results were obtained when the excitation wavelength was changed to 332 nm.

The time resolved decay measurements were carried out by single photon counting techniques, as described elsewhere.[11] Sample fluorescence was excited at 332 nm by a frequency-doubled (Inrad KDP′C′) 4-dicyanomethylene-2-methyl-6-(*p*-dimethylaminostyryl)-4*H*-pyran (DCM) jet stream dye laser (Spectra Physics Model 171) at a repetition rate of 4 MHz. Instrument response profiles were obtained as described before[11] by scattering the excitation light from solvent and changing delay times bases (ps per channel) were calculated. Analysis of the fluorescent decay was carried out using a non-linear least-squares-fitting program based on the Marquardt algorithm. Decay data fits monoexponential decay with χ^2 ranging from 1–1.2 for all experiments.

Quantum yield measurements

The fluorescence quantum yields of pyr–COOH (**1**) and *N*-pyr–L-Glu(OEt)–OEt (**2**) in dry acetonitrile were measured with reference to quinine sulfate ($\Phi_f = 0.546$ in 0.5 M H_2SO_4) as described before by comparing the area of fluorescence and absorbance using formula (1)[12] where Φ_{sample} and Φ_{std}, a_{sample} and a_{std}, η_{sample} and η_{std}, A_{sample} and A_{std} are the quantum yield, area under the emission spectra, refractive index of the solvent, and the absorbance of the samples under study (**1** and **2**) and the standard (quinine sulfate), respectively.

$$\Phi_{sample} = \frac{a_{sample}}{a_{std}} \times \frac{A_{std}}{A_{sample}} \times \frac{\eta_{sample}}{\eta_{std}} \times \Phi_{std} \qquad (1)$$

Study of molecular interactions of 2 and 4 by Job's method

Equimolar stock solutions of **2** and 4-(*N*–Boc-L-Glu(OH))–adma **4** (1 M) in $CDCl_3$ were prepared and then mixed to provide a series of 10 samples of varying mole fractions (x) of 0.9 to 0.1 of **4**. 250 μl of $CDCl_3$ were added to the NMR tube in order to give acceptable sample volumes. The chemical shifts of the amide protons of both species were monitored as a function of the x of **4**. The change in chemical shift multiplied by the mole fraction (x) of **4** was plotted *versus* x of **4**, according to Job's method modified for NMR by Blanda *et al.*[13] The stoichiometry of the resulting complex peptide complex is obtained from the Job plots as 1 : 1.

Electrochemical studies

All electrochemical experiments were carried out using a CV-50W Voltammetric Analyzer (BAS) in air at room temperature. The solvent was acetonitrile containing 0.1 mol tetrabutylammonium perchlorate (TBAP) as supporting electrolyte. For the cyclic voltammetry studies a glassy carbon working electrode (BAS, diameter 2 mm) and a platinum wire counter electrode were used. The reference electrode was a Ag/AgCl electrode (BAS). iR compensation was applied. Backgrounds of the solvent containing 0.1 M TBAP were collected before each set of experiments and then subtracted from the voltammograms.

Preparation of *N*-pyrenoyl-L-glutamic acid diethyl ester (2)

To a well stirred solution of pyrenecarboxylic acid (100 mg, 0.41 mmol) in CH_2Cl_2 (10 mL), HOBT (60 mg, 0.43 mmol) and DCC (87 mg, 0.42 mmol) were added. L-Glutamic acid diethyl ester hydrochloride was treated with Et_3N in CH_2Cl_2 and the mixture was added to the stirring slurry. Stirring was continued at room temperature for 24 h. It was then extracted successively with saturated sodium bicarbonate solution, 10% citric acid solution, again sodium bicarbonate solution and lastly with water. The organic phase was dried over $MgSO_4$ and evaporated *in vacuo*. The residue was then dissolved in minimum volume of CH_2Cl_2 and filtered and dried, giving a light yellow solid (138 mg, yield 83%). MW for $C_{26}H_{25}O_5N$: calc. 431.5; found 431.2. UV–Vis (λ_{max} in nm, ε in L cm^{-1} mol^{-1}): 275, 341 (2.25×10^4). ^{1}H-NMR (δ in ppm, $CDCl_3$): 8.69 (1H, d, H of pyrene), 8.19 (8H, m, H of aromatic pyrene), 6.91 (1H, d, $J_{HH} = 7.4$, NH of N-term), 5.03 (1H, m, CH Glu), 4.33 (2H, q, $J_{HH} = 7.3$, -OCH_2CH$_3$), 4.13 (2H, q, $J_{HH} = 7.2$, -OCH_2CH$_3$), 2.60 (2H, m, -CHCH_2- adjacent to asymmetric carbon), 2.41 (2H, m, CHCH$_2$CH_2-), 1.43 (3H, t, $J_{HH} = 7.5$, -OCH$_2$CH_3), 1.24 (3H, t, $J_{HH} = 7.5$, -OCH$_2$CH_3). ^{13}C-NMR (δ in ppm, $CDCl_3$): 173.2, 172.2 (C=O of OEt), 170.052 (C=O of pyr-CO-NH-), 132–124.5 (16 carbon of pyr), 62.1, 61.1 (2 *C*H$_2$ of OEt), 52.8 (asymmetric carbon of E), 30.98 (CH$_2$-*C*H$_2$-COOEt), 27.64 (*C*H$_2$-CH$_2$-COOEt), 14.45, 14.38 (CH$_3$ of OEt).

Preparation of *N*-Boc–L-Glu–(OBzl)–adma (3)

A well stirred, ice-cooled and argon saturated solution of activated ester of Boc–L-Glu–(OBzl)–OH [prepared from 1 mmol Boc–L-Glu–(OBzl)–OH (337 mg) and both 1.1 mmol HOBT (147 mg) and DCC (227 mg) in 20 ml of dry dichloromethane] was admixed with adma (1.1 mmol, 230 mg separately reacted with triethylamine in dichloromethane). The combined reaction mixture was stirred at room temperature for 24 h and kept in the dark. It was then extracted successively with saturated sodium bicarbonate solution, 10% citric acid solution, again sodium bicarbonate solution and lastly with water. The organic phase was dried over $MgSO_4$ and evaporated *in vacuo*. The residue was then dissolved in minimum volume of CH_2Cl_2 and filtered and dried. The colour of the product (the crude product: 351 mg, yield 64%) was off-white. MW for $C_{25}H_{34}O_5N_3$: calc. 456.56; found 455.25. UV–Vis (λ_{max} in nm, ε in L cm^{-1} mol^{-1}): 275 (2.5×10^5). ^{1}H-NMR (δ in ppm, $CDCl_3$): 8.26 (br s, NH of adma), 7.34 (5H, br d, OBzl-H, $J_{HH} = 9.0$), 6.67 (2H, d, Ph-H of adma, towards dimethylamine), 5.54 (d, NH of N-term, $J_{HH} = 7.8$), 5.13 (2H, s, CH$_2$ of OBzl), 4.34 (br s, CH asym), 2.91 (6H, s, CH$_3$ of dimethyl of adma), 2.56 (2H, d, G-CH$_2$), 2.23 (q, CH of Glu near asymmetric carbon), 2.05 (q, CH of Glu), 1.44 (9H, s, CH$_3$ of Boc). ^{13}C-NMR (δ in ppm, $CDCl_3$): 173.46 (C=O of OBzl), 169.62 (C=O of NH-adma), 156.2 (C=O of Boc), 148.3 (Ph carbon attached to NH of adma), 135.92 (Ph carbon attached to NMe$_2$ of adma), 128.8, 128.5, 127.64 (Ph carbons of OBzl), 121.94 (Ph carbon *ortho* to NH of adma), 113.23 (Ph carbon *meta* to NH of adma), 80.46 (tertiary carbon of Boc), 66.83 (CH$_2$ of OBzl), 54.412 (asymmetric carbon of E), 41.14 (2CH$_3$ of adma), 34.13 (-*C*H$_2$CO-OBzl), 28.55 (CH$_3$ of Boc), 25.17 (*C*H$_2$CH$_2$COOH of E).

Preparation of *N*-Boc–L-Glu(OH)–adma (4)

To an argon saturated solution of Boc–L-Glu(OBzl)–adma (200 mg, 0.43 mmol) in MeOH (50 ml) Pd/C (100 mg, 5% Pd) was added. Hydrogen gas was bubbled through the vigorously stirring slurry for 1 h. The progress of the reaction was followed by TLC (silica gel on Al, Riedel-de Haan, MeOH). After completion, the solution was purged with argon and filtered through a cotton pad. Evaporation of the filtrate gave an off-white solid (100 mg, 91%). UV–Vis (λ_{max} in nm, ε in L cm^{-1}

mol^{-1}): 275 (1.68×10^5). ^{1}H-NMR (δ in ppm, $CDCl_3$): 8.84 (s, NH of N-terminal), 7.39 (2H, d, Ph-H of adma, $J_{HH} = 9.0$), 6.65 (3H, d, overlapping signals of aromatic H of adma and OH of Glu), 5.52 (br s, NH C-terminal), 4.56 (br m, of CH Glu), 2.88 (6H, s, 2 CH_3 of adma), 2.47 (2H, m, CH_2 of Glu) 2.11 (2H, m, CH_2 of Glu), 1.43 (9H, s, 3 CH_3 of Boc). ^{13}C-NMR (δ in ppm, $CDCl_3$): 176.4 (C=O of free acid), 170.03 (C=O attached to adma), 156.43 (C=O attached to NH of E), 148.15 (Ph carbon attached to NH of adma), 128.12 (Ph carbon attached to NMe_2 of adma), 121.977 (Ph carbon *ortho* to NH of adma), 113.4 (Ph carbon *meta* to NH of adma), 80.6 (tertiary carbon of Boc), 54.1 (asymmetric carbon of E), 41.2 ($2CH_3$ of adma), 33.98 (-*C*H_2COOH of E), 28.54 (CH_3 of Boc), 25.1 (*C*H_2CH_2COOH of E).

Results and discussion

a. Synthesis and spectroscopic characterization

Coupling of pyrenecarboxylic acid (pyr, **1**) to bis-ethyl protected glutamic acid was achieved by reaction of the *in situ* generated active ester pyr–OBT, generated from **1** with 1-hydroxybenzotriazole (HOBT) and dicyclohexylcarbodiimide (DCC) in CH_2Cl_2, with the protected amino acid (Scheme 1) according to common peptide coupling techniques.[9]

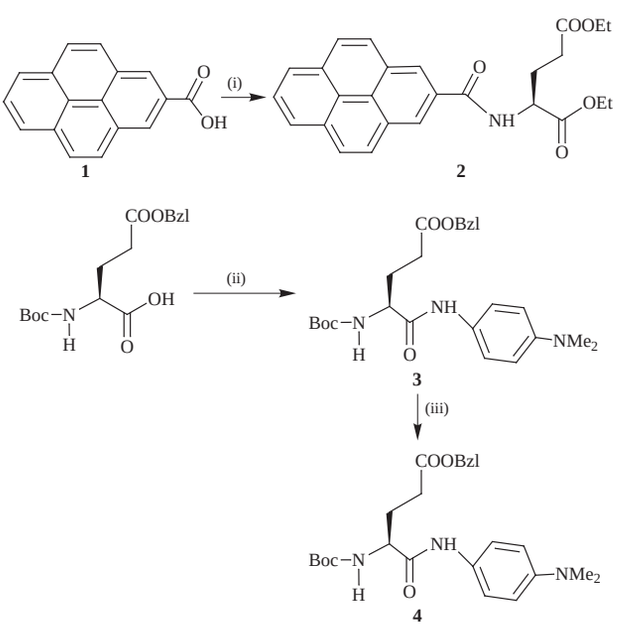

Scheme 1 Synthesis of pyrenoyl glutamic acids ester and 4-(Boc–glutamide)–*N*,*N*-dimethylaniline; (i) H–E(OET)–OET, Et_3N, DCC, HOBT, CH_2Cl_2; (ii) adma·2HCl, xs Et_3N, DCC, HOBT, CH_2Cl_2; (iii) Pd/C, H_2, MeOH.

The reaction of Boc–glutamic acid with free 4-amino-*N*,*N*-dimethylaniline (adma) dihydrochloride in dichloromethane in the presence of excess triethylamine cleanly gives the desired benzyl protected product *N*-Boc–L-Glu(OBzl)–adma (**3**) as an off-white solid in 64% yield (Scheme 1). **3** is only moderately air-sensitive in the solid state. It is important to stress at this point that the same compound obtained from the reactions using free 4-amino-*N*,*N*-dimethylaniline (commercially available from Aldrich) results in the formation of reddish materials. The reddish impurity, most likely the oxidized aniline, could not be removed despite repeated recrystallizations. The benzyl group is easily removed by hydrogenation over Pd/C to give *N*-Boc–L-Glu(OH)–adma (**4**). Solutions of **4** rapidly will turn red in the presence of oxygen and have to be stored in the dark under an inert atmosphere. All compounds were characterized by NMR and mass spectroscopy. The amide resonance of **2** (δ 6.91) compares well with other modified glutamic acid derivatives.[9c] **3** and **4** exhibit two amide resonances due to the Boc-NH (**3**: δ 5.54; **4**: δ 5.52) and the adma amide (**3**: δ 8.26; **4**: δ 8.84).

b. Molecular interactions

1–**4** have the possibility to form H-bonded complexes in solution *via* interaction of several possible combinations of amide and carbonyl groups. We decided to study the interaction of **2** and **4** in detail. For **2** and **4**, H-bonding can involve the backbone amides and carbonyls, as well as the ester carbonyls of **2** and the carboxylic sidechain of **4**, allowing several possible H-bonding interactions. We show only three possible H-bonding interactions (**I**–**III**).

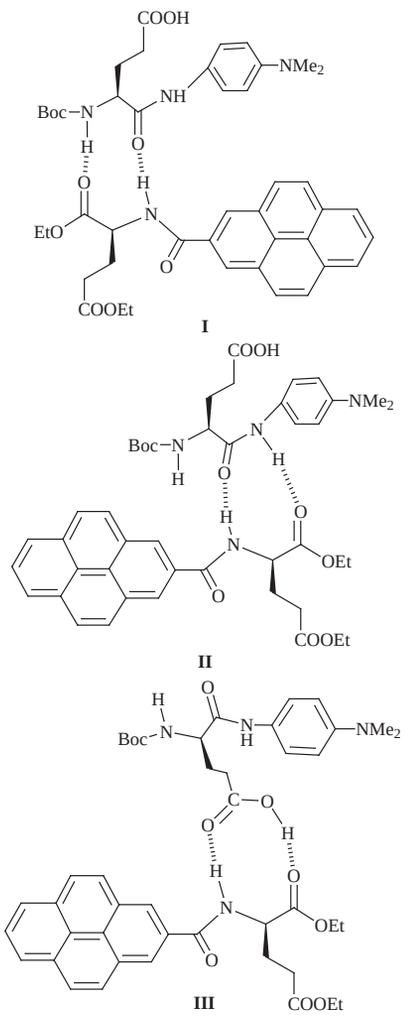

Chart 2

IR studies monitoring the ν_{CO} of **2** and **4** were inconclusive. However, molecular interactions involving amino acids or peptides can be conveniently monitored by ^{1}H NMR spectroscopy. Hydrogen bonding interaction between the fluorophore and the quencher should cause shifts in the peak positions of the amide protons of both molecules. Hence, we decided to carry out an NMR titration experiment[12] in non-protic $CDCl_3$ in order to evaluate the ability of **2** and **4** to form H-bonded complexes and to determine if the backbone is involved in H-bonding. In this experiment, we monitored the shifts of the proton resonances that occur upon mixing of the two species. We find that only the amide protons of **2** and **4** exhibit shifts in the NMR spectrum, indicating their involvement in hydrogen bonding. Other resonances remain unchanged. Addition of a solution of **2** to a solution of **4** causes downfield shifts in the NH resonance of **2** from δ 6.91 ($x = 1$) to δ 6.93 ($x = 0.1$), giving a maximum $\Delta\delta$ of only 0.02 ppm, indicating an interaction

at this proton. The adma amide resonance of **4**, on the other hand, undergoes an upfield shift from δ 8.84 (for a neat solution of **4**) to δ 8.70 ($x = 0.2$ of **4**), indicating that this proton is involved in some form of H-bonding. The Boc-NH of **4** exhibits an upfield shift from δ 5.52 to δ 5.45 ($x = 1$ and $x = 0.2$, respectively). The observed shifts for this system are small compared to other systems known to undergo a very strong H-bonding,[14] indicating that H-bonding between **2** and **4** is weak and most likely non-specific.

The Job plot (Fig. 1), constructed from the NMR titration experiments monitoring the amide resonance of **4**, shows a maximum at $x = 0.5$, corresponding to a 1:1 stoichiometry for the complex. Further indications of the weak interaction come from association constants measured by fluorescence spectroscopy (*vide infra*).

c. Absorption and fluorescence studies

As expected, the UV–Vis spectrum of **2** exhibits virtually identical absorption bands compared to pyrene-1-carboxylic acid (**1**) with a slight blue-shift of the bands (Fig. 2). **3** and **4** possess a single absorption at 275 nm. Mixing of **3** and **4** with **1** or **2** do not give rise to any new or shifted bands. The extinction coefficients of **1** and **2** have been listed in Table 1. Quantum yield (φ) measurements[12] show that the quantum yield of **2** is only half of that of **1** (Table 1).

The fluorescence quenching behavior[15] of **1** and **2** with **3** and **4** was studied in various solvents. From the structures of compounds **1** to **4**, it is evident that both the acceptors (**1**, **2**) and donors (**3**, **4**) have several H-bonding sites, ranging from backbone amide and carbonyl to ester and acid sidechains. In non-protic solvents there is a high propensity for formation of an inter- or intramolecular H-bonded complex between fluorophore and quencher as described above. The absorption and excitation spectra of **2** are identical, making it unlikely that intramolecular H-bonded complexes are formed.

In order to evaluate the fluorescence quenching taking place in an H-bonded complex of fluorophore and quencher in solution, we carried out a steady-state fluorescence study of **1** and **2** with **3** and **4**. Stern–Volmer (SV) plots have been constructed by plotting F_0/F *vs.* [Q],[15] using relationship (2),

$$F_0/F = 1 + K_{sv}[Q] \quad (2)$$

where F_0 and F are fluorescence intensities in the absence and presence of quenchers respectively, and K_{sv} is the SV quenching constant. The steady-state fluorescence quenching studies show

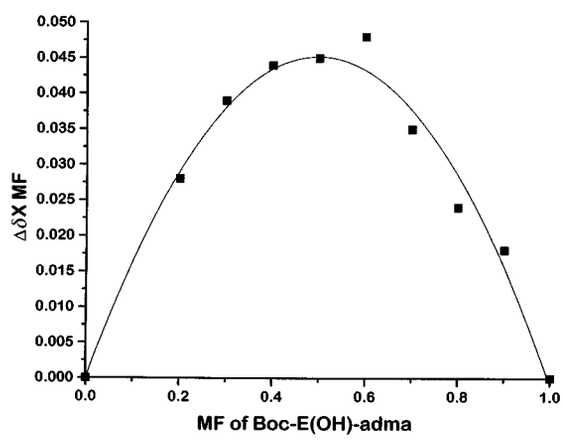

Fig. 1 ^{1}H-NMR Job plot for the interaction of **2** and **4** in $CDCl_3$. The concentrations of **2** and **4** were varied from 1.3×10^{-3} to 1.3×10^{-2} mol dm^{-3}. Monitored is the amide resonance of **4**. The solid line represents the curve fit.

Table 1 Photophysical data of **1** and **2** in acetonitrile

Compound	λ^a_{abs}/nm	ε_{max}/M^{-1} cm^{-1}	λ^b_{em}/nm	φ	τ_0/ns
1	349	2.5×10^4	387	0.78	6.9 ± 0.08
2	341	2.2×10^4	382	0.39	13.9 ± 0.1

λ^a_{abs} = absorption maxima, ε_{max} = extinction coefficient at λ^a_{abs}, φ = fluorescence quantum yield, τ_0 = lifetime of the fluorophore.

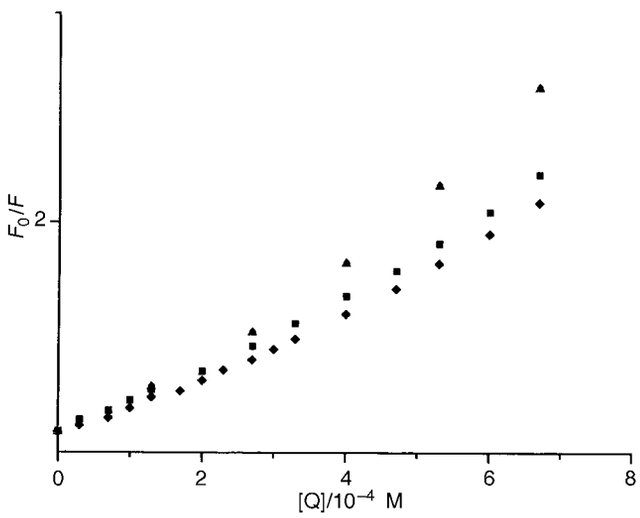

Fig. 3 Steady-state Stern–Volmer quenching of **1** [3.33×10^{-6} mol dm^{-3}] and **2** [3.33×10^{-6} mol dm^{-3}] by **3** and **4** in acetonitrile. The concentrations of **3** and **4** are varied from 0–4.0×10^{-4} mol dm^{-3}. F_0 and F are the intensities of the fluorescence of the fluorophores in the absence and presence of quenchers and [Q] is the concentration of the quenchers **3** and **4**, respectively. (■ 2/4; ▲ 1/3; ◆ 1/4; ● 2/3). Curves for 2/3 (●) and 1/3 (▲) are virtually identical.

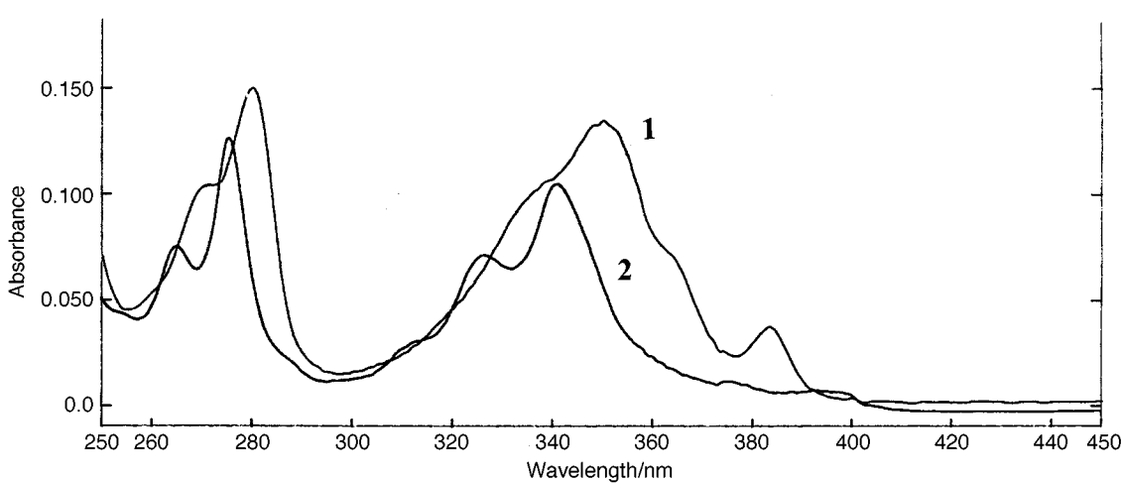

Fig. 2 Absorption spectra of **1** (top) and **2** (bottom) in dry acetonitrile. Both are at equimolar concentrations (6.67×10^{-6} mol dm^{-3}).

Table 2 Association constants, K_{as}, and bimolecular quenching constants, k_q, of the four pairs of acceptor–donor systems in acetonitrile

System	$K_{as}/\times 10^3\ M^{-1}$	$k_q/M^{-1}\ s^{-1}\times 10^{10}$	$\ln k_q$
1–**4**	3.8 ± 0.11	1.26	23.26
2–**4**	4.0 ± 0.08	1.0	23.03
1–**3**	3.79 ± 0.07	1.28	23.27
2–**3**	3.79 ± 0.08	1.1	23.12

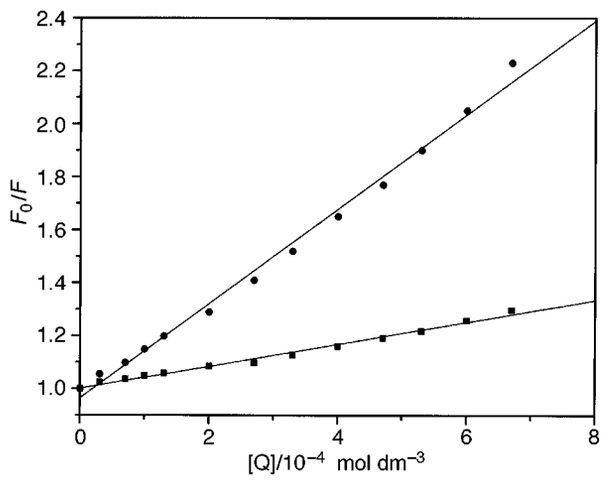

Fig. 4 Quenching of **2** [6.67×10^{-6} mol dm^{-3}] with **4** in wet (■) and dry (●) acetonitrile. The concentration of **4** was varied from 0–1.33×10^{-4} mol dm^{-3}.

a rapid quenching with an upward bending of the SV plots (Fig. 3), which is due to the presence of both static and dynamic quenching processes.[16]

In dry acetonitrile, steady-state fluorescence experiments are consistent with a unimolecular quenching reaction of the fluorophores, with an association constant K_{as} ranging from 3.7×10^3 to 4×10^3 M^{-1} (see Table 2). Importantly, we did not observe significantly higher K_{as} for systems able to undergo multiple H-bonding involving the Glu acid sidechain (**1**–**4** and **2**–**4**). From the values of the association constant it is clear that there may be a weak interaction between the acceptor **2** and the donor **4**, however for specific and multiple site H-bonding K_{as} of 10^6 M^{-1} is common.[5] This may imply that the acid sidechain in **4** is not involved in binding to the peptide backbone, and that interaction **C** is weak. This is in accord with our NMR results, which suggests that the backbone amides of **2** and **4** are involved in the interaction between the two species.

We then proceeded to evaluate the effects of intermolecular H-bonding of the fluorophores **1** and **2** with the solvent. The quenching abilities of **3** and **4** in wet acetonitrile are significantly lower, most likely due to the formation of new H-bonded species involving water (Fig. 4).

We observe that upon addition of a small amount of water to rigorously dried acetonitrile (v/v 50:1), the fluorescence intensity of **1** and **2** is slightly decreased even before the addition of any quencher, suggesting the formation of an aquo-complex in solution. In separate experiments, we found that addition of **3** or **4** to solutions of **1** and **2** in methanol and ethanol result in an initial large increase of fluorescence intensity, which then decreases upon further addition of quencher. This behavior is compatible with the disruption of H-bonding between the solvent and the fluorophore by the quencher, followed by rapid quenching. This is in accord with previously observed environmental influences on fluorescence intensities.[17] Hence, protic solvents will form an H-bonded solvent sphere around the fluorophore. This reduces the probability of formation of an H-bonded complex between the fluorophore and the quencher in the ground state and thus the

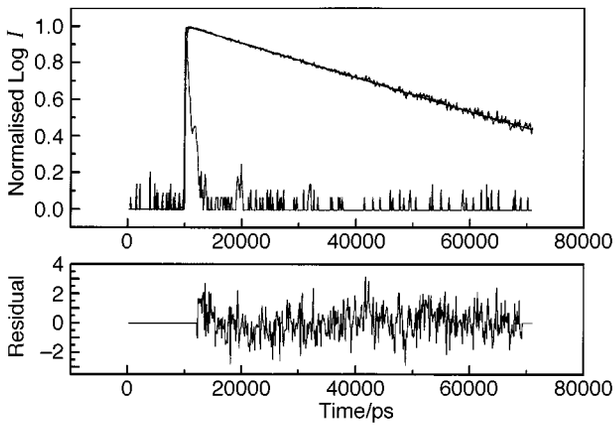

Fig. 5 Decay profile of **2** [6.67×10^{-6} mol dm^{-3}] in dry acetonitrile.

fluorescence quenching will be drastically reduced due to inaccessibility of the fluorophore by the quencher.[17]

In the absence of quencher, the lifetimes of **1** and **2** in dry acetonitrile are 6.9 and 13.9 ns, respectively. The decay profile for **2** is shown in Fig. 5.

We then proceeded to study the dynamic quenching behavior by lifetime measurements and thereby understand the upward bending in the steady-state SV plots (*vide supra*). The dynamic portion of the quenching can be determined from the lifetime measurements following eqn. (3),[15] where τ_0 and τ are

$$\tau_0/\tau = 1 + k_q\tau_0\,[Q] = 1 + K_D[Q] \qquad (3)$$

fluorescence lifetimes in the absence and presence of quenchers respectively, and K_D is the SV quenching constant. The lifetime studies of the fluorophores **1** and **2** in the presence of increasing concentrations of quenchers **3** and **4** result in linear SV plots (Fig. 6), in accord with a dynamic quenching process.

The bimolecular quenching constants k_q have been calculated (K_D/τ_0) and are listed in Table 2. The bimolecular quenching constants are similar in all cases. The bimolecular quenching constant k_q for all acceptor–donor pairs is in the range 1.0–1.28×10^{10} s^{-1}, which is in the region of diffusion controlled forward electron transfer processes (*vide infra*).[18]

This observation indicates that the rate of electron transfer from the fluorophore to the quencher is unaltered and is independent of sidechain protection. Though steady-state fluorescence and NMR data clearly indicate the formation of an H-bonded complex, we conclude that the sidechain is not involved in formation of H-bonding. Rather, our data support formation of a complex where only the backbone amide and carbonyls are responsible for weak H-bonding. To ascertain the role of H-bonding in electron transfer, future studies will be aimed at designing systems allowing for a more specific H-bonding interaction between donor and acceptor moieties.

In order to get an indication of the quality of our measurement, we carried out a theoretical calculation of the electron transfer rate constant k_q, taking into consideration the redox potentials of the fluorophore and the quenchers.

Outer-sphere electron transfer quenching can be expressed by the Rehm–Weller eqn. (4),[19] where $K_d = k_d/k_{-d}$, k_d is the

$$k_q = \frac{k_d}{1 + (k_d/\nu K_d)\exp(\Delta G_{el}^{\ddagger}/RT)} \qquad (4)$$

diffusion rate constant for the forward reaction, ν is the frequency factor and $\Delta G_{el}^{\ddagger}$ is the Gibbs energy of activation for the electron transfer step. According to Marcus theory, $\Delta G_{el}^{\ddagger}$ can be related to the change in free energy ΔG^0 and the reorganizational energy λ according to eqn. (5).[20] ΔG^0 can be related to

$$\Delta G_{el}^{\ddagger} = (\lambda/4)(1 + \Delta G^0/\lambda)^2 \qquad (5)$$

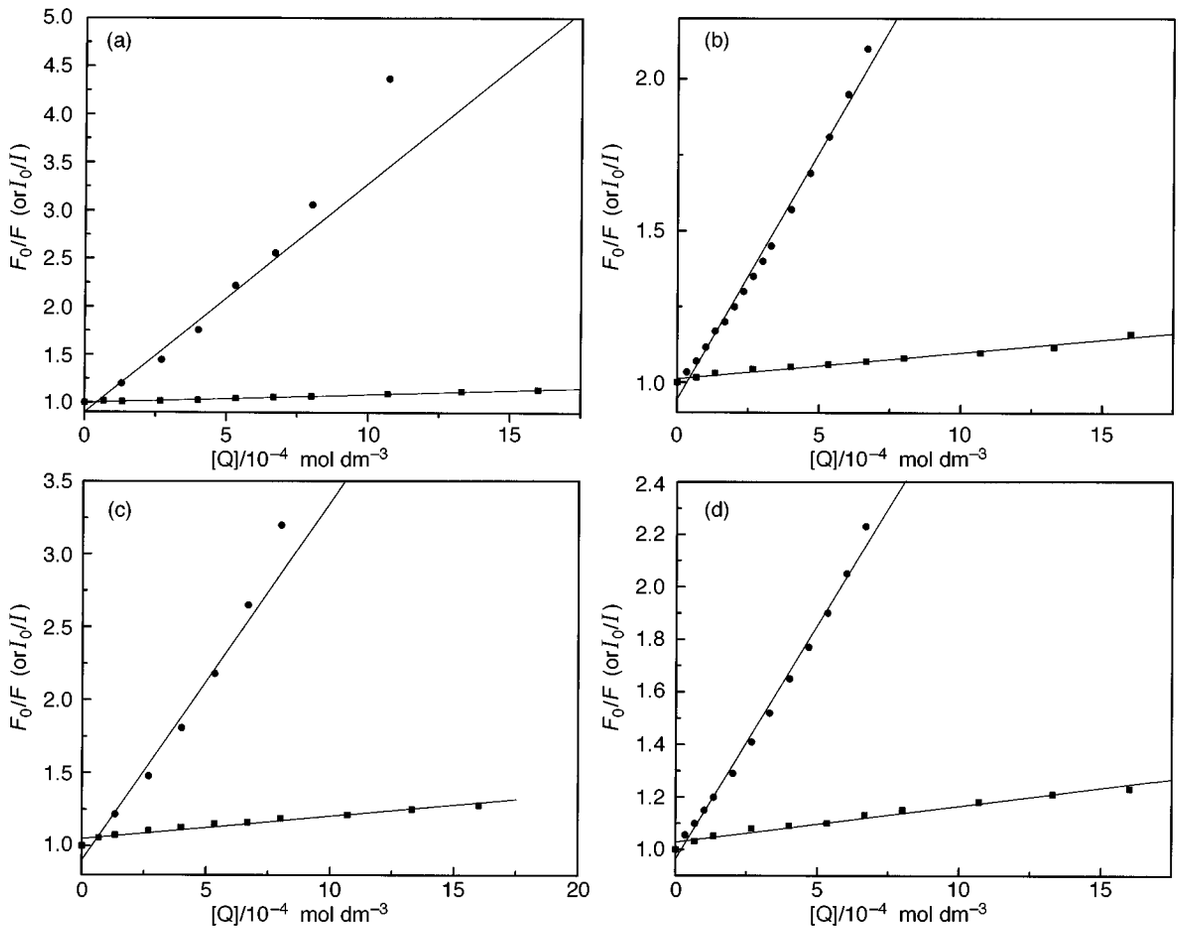

Fig. 6 Stern–Volmer quenching plots obtained from steady-state (●) and lifetime (■) measurements between **1** and **3** (a), **1** and **4** (b), **2** and **3** (c) and **2** and **4** (d) in dry acetonitrile. The concentration of **1** and **2** is 3.33×10^{-6} mol dm^{-3}. The concentrations of **3** and **4** were varied from 0–1.6×10^{-3} mol dm^{-3} for the lifetime measurements and from 0–6.67×10^{-4} mol dm^{-3}.

the change in free energy between the ground state D + A and the excited state $D^+ + A^-$ and can be calculated according to eqn. (6),[8b] where $E^0(D/D^+)$ and $E^0(A/A^-)$ are the standard

$$\Delta G^0 = [E^0 (D/D^+) - E^0 (A/A^-) - E_{0\text{–}0} - e^2/\varepsilon r] \quad (6)$$

reduction potentials of donor and acceptor, respectively. $E_{0\text{–}0}$ is the 0–0 excitation energy of the fluorophore, which is obtained from the cross-over point of the excitation and emission spectra of the fluorophore. ε is the permittivity of the solvent and e^2/r is the Coulombic interaction for radical ions at distance r. In acetonitrile solution, the last term is small and can be omitted.[8b] We have measured the reduction potentials of **3** and **4** in dry acetonitrile to be +0.85 V (*vs.* NHE) and +0.86 (*vs.* NHE), respectively. These compare well to the literature value of +0.81 V for free adma.[21] Precise values for the reduction potentials of **1** and **2** were not obtained and were estimated to be close to that of pyrene-3-carboxylic acid (−1.67 V).[19] This gives us a driving force for electron transfer from **3** and **4** to **1** and **2** ranging from $\Delta G^0 = -0.77$ to −0.84 eV. This falls within the normal Marcus region indicating forward electron transfer.[10,19] From this ln k_q can be estimated to 22.2,[22] which compares favorably with our experimental values ranging from ln k_q of 23.03–23.27 (Table 2).

Summary and outlook

The importance of the H-bonded interface in biological ET processes has been addressed for non-peptidic model systems experimentally.[3–5] We set out to evaluate the role of H-bonding in ET processes using glutamic acid derivatives by studying the fluorescent lifetime of fluorophore- and quencher-labeled glutamic acid. The DCC–HOBT protocol provides a convenient method for the preparation of *N*-pyrenoyl glutamic acid ester and Boc–glutamide-*N*,*N*-dimethylaniline ester. Whereas there are several possibilities for peptidic systems to interact by H-bonding (Chart 1), NMR spectroscopic studies of our modified glutamic acid derivatives clearly show that there is only a weak non-specific H-bonding interaction between fluorophore- and quencher-labeled glutamic acids. Association constants for all systems investigated, determined by fluorescence methods, are in the order of 3.8–4.0×10^3 M^{-1}. From measurements of the fluorescent lifetime of the fluorophore in the presence and absence of *N*-Boc–L-Glu(OR)–adma (R = H, Bzl), we obtained bimolecular quenching constants k_q that are in the order of 1.0×10^{10} M^{-1} s^{-1}, indicating a diffusion controlled ET process. Since the rate of ET remains virtually unchanged, we conclude that the weak and non-specific H-bonding present in our systems does not provide a specific pathway for more effective ET. However, we will continue our research into ET across the H-bonded peptidic interface, designing systems able to undergo stronger and more specific H-bonding interactions, such as arginine and glutamic acid based systems forming a strong salt bridge.

Acknowledgements

We thank the Department of Chemistry for financial support. This work was supported in part by the Samuel and Ethel Brown Memorial Fund. H. B. K. wishes to thank the University of Saskatchewan for an NSERC President's Award. We also wish to thank Professor R. P. Steer for the use of his spectroscopic equipment.

References

1 I. Bertini, H. B. Gray, S. J. Lippard and J. S. Valentine, *Bioinorganic Chemistry*, University Science Books, Mill Valley, CA, 1994.

2 (*a*) D. N. Beratan, J. N. Betts and J. N. Onuchic, *Science*, 1991, **252**, 1285; (*b*) S. S. Skourtis and D. N. Beratan, *J. Biol. Inorg. Chem.*, 1997, **2**, 378; (*c*) R. J. P. Williams, *J. Biol. Inorg. Chem.*, 1997, **2**, 373 and references therein.

3 P. J. F. de Rege, S. A. Williams and M. J. Therien, *Science*, 1995, **269**, 1409.

4 (*a*) C. Turró, C. K. Chang, G. E. Leroi, R. I. Cukier and D. G. Nocera, *J. Am. Chem. Soc.*, 1992, **114**, 4013; (*b*) J. M. Zaleski, C. Turró, R. D. Mussel and D. G. Nocera, *Coord. Chem. Rev.*, 1994, **132**, 249; (*c*) J. A. Roberts, J. P. Kirby and D. G. Nocera, *J. Am. Chem. Soc.*, 1995, **117**, 8051; (*d*) J. P. Kirby, N. A. van Dantzig, C. K. Chang and D. G. Nocera, *Tetrahedron Lett.*, 1995, **36**, 3477.

5 P. Tecilla, R. P. Dixon, G. Slobodkin, D. S. Alavi, D. H. Waldeck and A. D. Hamilton, *J. Am. Chem. Soc.*, 1990, **112**, 9408.

6 For example: (*a*) S. S. Isied, M. Y. Ogawa and J. F. Wieshart, *Chem. Rev.*, 1992, **92**, 381; (*b*) A. K. Mishra, R. Chandrasekar, M. Faraggi and M. H. Klapper, *J. Am. Chem. Soc.*, 1994, **116**, 1414 and references therein; (*c*) M. A. Fox and E. J. Galoppini, *J. Am. Chem. Soc.*, 1997, **119**, 5277; (*d*) K. S. Schanze and K. Sauer, *J. Am. Chem. Soc.*, 1988, **110**, 1180; (*e*) G. Basu, M. Kubasik, D. Anglos, B. Secor and A. Kuki, *J. Am. Chem. Soc.*, 1990, **112**, 9410; (*f*) S. L. Mecklenburg, B. M. Peek, J. R. Schoonover, D. G. McCafferty, C. G. Wall, B. W. Erickson and T. J. Meyer, *J. Am. Chem. Soc.*, 1993, **115**, 5479 and references therein; (*g*) T. Hayashi, T. Takimura, Y. Hitomi, T. Ohara and H. Ogoshi, *J. Chem. Soc.*, *Chem. Commun.*, 1995, 545.

7 T. E. Creighton, *Proteins: Structures and Molecular Properties*, 2nd edn., W. H. Freeman, New York, 1993.

8 (*a*) Y. Taniguchi, Y. Nishina and N. Mataga, *Bull. Chem. Soc. Jpn.*, 1972, **45**, 746; (*b*) G. J. Kavarnos and N. J. Turro, *Chem. Rev.*, 1986, **86**, 401.

9 (*a*) M. Bodanszky and A. Bodanszky, *The Practice of Peptide Synthesis*, Springer Verlag, Berlin, 1984; (*b*) D. H. Rich and J. Singh, in *The Peptides I*, E. Gross and J. Meienhofer (ed.), ch. 5, Academic Press, New York, 1979; (*c*) H.-B. Kraatz, J. Lusztyk and G. D. Enright, *Inorg. Chem.*, 1997, **36**, 2400 and references therein.

10 R. A. Marcus, *J. Chem. Phys.*, 1956, **24**, 966.

11 D. R. James, D. R. M. Demmer, R. E. Verrall and R. P. Steer, *Rev. Sci. Instrum.*, 1983, **54**, 1121.

12 S. Aich, C. Raha and S. Basu, *J. Chem. Soc.*, *Faraday Trans.*, 1997, **93**, 2991.

13 M. T. Blanda, J. H. Horner and M. Newcomb, *J. Org. Chem.*, 1989, **54**, 4626.

14 C. N. Kirsten and T. H. Schrader, *J. Am. Chem. Soc.*, 1997, **119**, 12 061.

15 J. R. Lakowicz, *Principles of Fluorescence Spectroscopy*, ch. 9, Plenum Press, New York, 1983.

16 Static quenching is not easily identifiable from the absorption studies of fluorophore mixed with quenchers.

17 E. L. Wehry, in *Practical Fluorescence*, 2nd edn., ch. 3, G. G. Guilbault (ed.), Marcel Dekker, New York, 1990.

18 At this point we want to stress that energy transfer can be discarded in this study as there is no overlapping between the absorption bands of the quenchers with the emission bands of the fluorophores which is the basic requirement of energy transfer *i.e.*, $\cong E_{DA} > 0$.

19 D. Rehm and A. Weller, *Isr. J. Chem.*, 1970, **8**, 259.

20 (*a*) J.-M. Chen, T.-I. Ho and C.-Y. Mou, *J. Phys. Chem.*, 1990, **94**, 2889; (*b*) H. Pal, D. K. Palit, T. Mukherjee and J. P. Mittal, *J. Chem. Soc.*, *Faraday Trans.*, 1993, **89**, 683.

21 D. G. Nocera and H. B. Gray, *J. Am. Chem. Soc.*, 1981, **103**, 7349.

22 This value was calculated from previously measured values of pyrene-3-carboxylic acid of −1.67 V (ref. 18) and our measured values for **3** and **4**.

Paper 8/05907A